▌Photoinitiators |*Hot Paper*|

Synthesis of Mixed-Functionalized Tetraacylgermanes

Sabrina D. Püschmann,[a] Philipp Frühwirt,[b] Michael Pillinger,[a] Andreas Knöchl,[a] Marlene Mikusch,[a] Judith Radebner,[a] Ana Torvisco,[a] Roland C. Fischer,[a] Norbert Moszner,[c] Georg Gescheidt,[b] and Michael Haas*[a]

Abstract: Tetraacylgermanes are known as highly efficient photoinitiators. Herein, the synthesis of mixed tetraacylgermanes **4a–c** and **6a–e** with a nonsymmetric substitution pattern is presented. Germenolates are crucial intermediates of these new synthetic protocols. The synthesized compounds show increased solubility compared with symmetrically substituted tetraacylgermanes **1a–d**. Moreover, these mixed derivatives reveal broadened n–π* absorption bands, which enhance their photoactivity. Higher absorption of these new compounds at wavelengths above 450 nm causes efficient photobleaching when using an LED emitting at 470 nm. The quantum yields are in the range of 0.15–0.57, depending on the nature of the aroyl substituents. On the basis of these properties, mixed-functionalized tetraacylgermanes serve as ideal photoinitiators in various applications, especially in those requiring high penetration depth. The synthesized compounds were characterized by elemental analysis, IR spectroscopy, NMR and CIDNP spectroscopy, UV/Vis spectroscopy, photolysis experiments, and X-ray crystallography. The CIDNP data suggest that the germyl radicals generated from the new tetraacylgermanes preferentially add to the tail of the monomer butyl acrylate. In the case of **6a–e** only the mesitoyl groups are cleaved off, whereas for **4a–c** both the mesitoyl and the aroyl group are subject to α-cleavage.

Introduction

Nowadays, photoinitiators (PIs)[1] are of high interest in different industrial applications, such as 3D printing,[2,3] coatings,[4] and in the medical sector for artificial tissues or dental filler materials.[5,6] The design and implementation of such PIs are very challenging. Requirements such as low toxicity, sustainability, environmental compatibility, low cost, and the fast

[a] Dipl.-Ing. S. D. Püschmann, M. Pillinger, A. Knöchl, M. Mikusch, Dr. J. Radebner, Dr. A. Torvisco, Prof. R. C. Fischer, Dr. M. Haas
Institute of Inorganic Chemistry
Technical University Graz
Stremayrgasse 9/IV, 8010 Graz (Austria)
E-mail: michael.haas@tugraz.at

[b] P. Frühwirt, Prof. Dr. G. Gescheidt
Institute of Physical and Theoretical Chemistry
Technical University Graz
Stremayrgasse 9/II, 8010 Graz (Austria)

[c] Prof. N. Moszner
Ivoclar Vivadent AG
Bendererstrasse 2, 9494 Schaan (Liechtenstein)

bleaching are crucial.[7] Photoinitiators can be classified as type I, type II, or multicomponent PIs.[8]

Recently, germanium-based photoinitiators have attracted considerable attention due to their low toxicity and bathochromic shift in their longest-wavelength absorption. Thus, they are promising alternatives to the currently widely used phosphorus-based photoinitiators.[9] However, the low abundance of germanium in the earth's crust results in higher costs. Di(4-methoxybenzoyl)diethylgermane (Ivocerin), a commercially available photoinitiator based on germanium, is synthesized via a multistep pathway.[10] This complex procedure, which relies on a Corey–Seebach reaction followed by column chromatography, results in the high cost of this PI. Another disadvantage is the inefficient curing depth at wavelengths above 500 nm.[11] We have introduced a new one-pot synthetic protocol providing tetraacylgermanes $Ge[C(O)R]_4$ (R=aryl) in high yields.[12] Furthermore, we found that tetraacylgermanes are more efficient photoinitiators than Ivocerin. Due to the presence of four RC=O chromophores, tetraacylgermanes show increased band intensities, which lead to more efficient light absorption. Different substituents on the aromatic ring allow tuning of the properties and shifting of the absorption band to higher wavelengths, which is ideal for medical applications. However, a huge drawback of symmetrical tetraacylgermanes are their high melting points, which are responsible for low solubility, limiting the field of applications.

Herein, we introduce two one-pot synthetic pathways to mixed-functionalized acylgermanes. The introduction of different substituents on the germanium center leads to increased
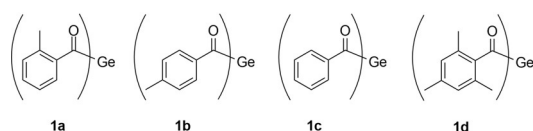
Chemistry–A European Journal

Full Paper
doi.org/10.1002/chem.202004342

Chemistry Europe
European Chemical
Societies Publishing

**Scheme 1.** Chemical structures of symmetrical tetraacylgermanes **1 a–d**.

solubility compared with symmetrical tetraacylgermanes **1 a–d** (Scheme 1). The broad absorption bands of these compounds promise a wide variety of applications.
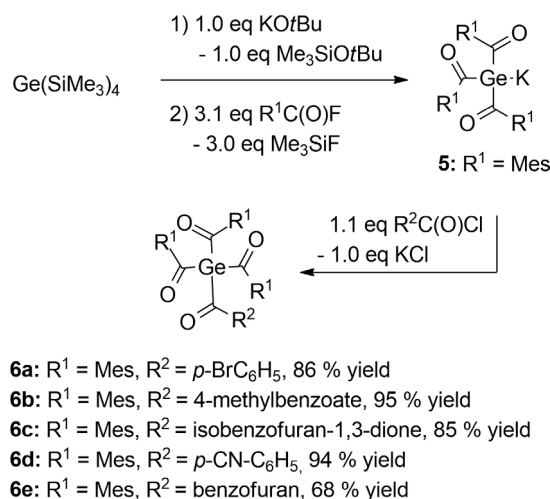
Results and Discussion

Introduction of mixed functionality

Method A

The entry into this chemistry is provided by tris(trimethylsilyl)acylgermane **2**, conveniently obtainable by reaction of tetrakis(trimethylsilyl)germane with equimolar amounts of KOtBu and acid chloride. Subsequently, **2** was treated with equimolar amounts of KOtBu generating the crucial germenolate intermediate **3**. To this germenolate a threefold excess of the respective acid fluoride was added in situ to yield the desired nonsymmetric products **4 a–c** in good yields. The reaction pathway is shown in Scheme 2. So far, this method turned out
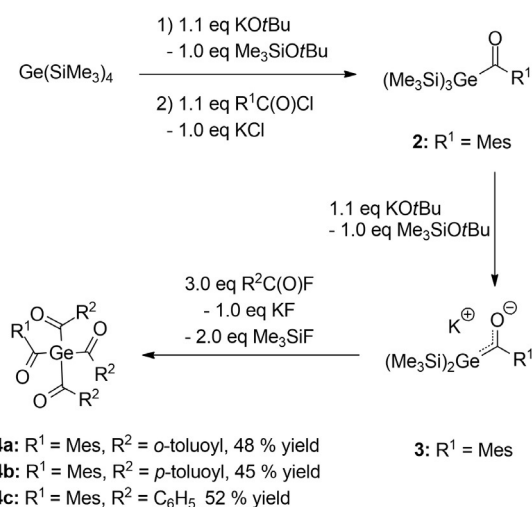
Scheme 2. Reaction scheme of method A. Synthesis of mixed-functionalized tetraacylgermanes **4 a–c**.

4a: R^1 = Mes, R^2 = o-toluoyl, 48 % yield
4b: R^1 = Mes, R^2 = p-toluoyl, 45 % yield
4c: R^1 = Mes, R^2 = C$_6$H$_5$, 52 % yield

to be restricted to electron-donating groups, while the introduction of electron-withdrawing groups (EWGs) was not possible. Due to the introduction of mixed functionality, the solubility increases drastically, but isolation of a clean product is more complex, and hence yields are reduced.

5: R^1 = Mes

6a: R^1 = Mes, R^2 = p-BrC$_6$H$_5$, 86 % yield
6b: R^1 = Mes, R^2 = 4-methylbenzoate, 95 % yield
6c: R^1 = Mes, R^2 = isobenzofuran-1,3-dione, 85 % yield
6d: R^1 = Mes, R^2 = p-CN-C$_6$H$_5$, 94 % yield
6e: R^1 = Mes, R^2 = benzofuran, 68 % yield

Scheme 3. Reaction scheme of method B. Synthesis of mixed-functionalized tetraacylgermanes **6 a–e**.

Method B

The starting material for method B (Scheme 3) is tetrakis(trimethylsilyl)germane. By adding equimolar amounts of KOtBu and subsequently 3.1 equiv of mesitoyl fluoride, the stable germenolate intermediate **5** is formed. This reaction could be accomplished via different synthetic routes,[13] but the direct method with KOtBu and mesitoyl fluoride used for this work generally gives higher yields. After the addition of KOtBu, the reaction solution turns yellow, which indicates consumption of KOtBu and the formation of the potassium germanide (Scheme 3). On adding a threefold excess of mesitoyl fluoride the solution turns reddish, which marks the formation of **5**. To the formed germenolate the corresponding acid chlorides were added in situ, and the desired products **6 a–d** were isolated in good to excellent yields. A huge advantage of this method is that EWGs can also be introduced. Consequently, this leads to a significant bathochromic shift and tailing of the longest wavelength absorption.
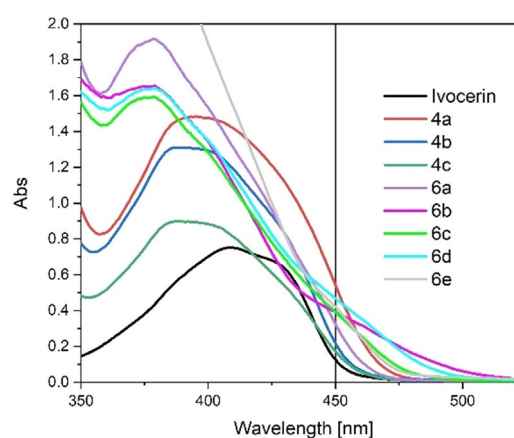
Figure 1. Absorption spectra of mixed-functionalized tetraacylgermanes compared with that of the commercially available Ivocerin with a concentration of 1×10^{-3} M in acetonitrile.

Chemistry–A European Journal

Full Paper
doi.org/10.1002/chem.202004342

Chemistry Europe
European Chemical
Societies Publishing

UV/Vis absorption spectra

The broad absorption band of each compound centered at about 390 nm (see Figure 1), attributed to the n–π* transition, is responsible for the photoinduced cleavage of the Ge–C bond. Importantly, these bands extend to >450 nm and show higher absorbance than that of the commercial PI, Ivocerin. Mesitoyltris(o-toluoyl)germane (**4a**) shows the highest absorption at this wavelength (tailing up to 475 nm) and could therefore play an important role in the medical industry. With **6b** tailing up to even 525 nm is obtained.

As shown in Figure 2a–c, the presence of one mesitoyl group leads to a hypsochromic shift on the one hand. On the other hand, more importantly, the extinction coefficient is increased, which leads to higher efficiency in light absorption. As depicted in Figure 2a–c, the absorption bands of the mixed-functionalized tetraacylgermanes are broader than those of the symmetrical ones. Therefore, excitation can be accomplished in a wider wavelength range, even at slightly higher wavelengths relative to the symmetrical acylgermanes. The only exception is mesitoyltribenzoylgermane (**4c**) (see Figure 2c). Tetraacylgermanes with EWGs show extended tailing

of the absorption above 500 nm (see Figure 2d). In general, the mixed derivatives show higher extinction coefficients than the symmetrical compounds.
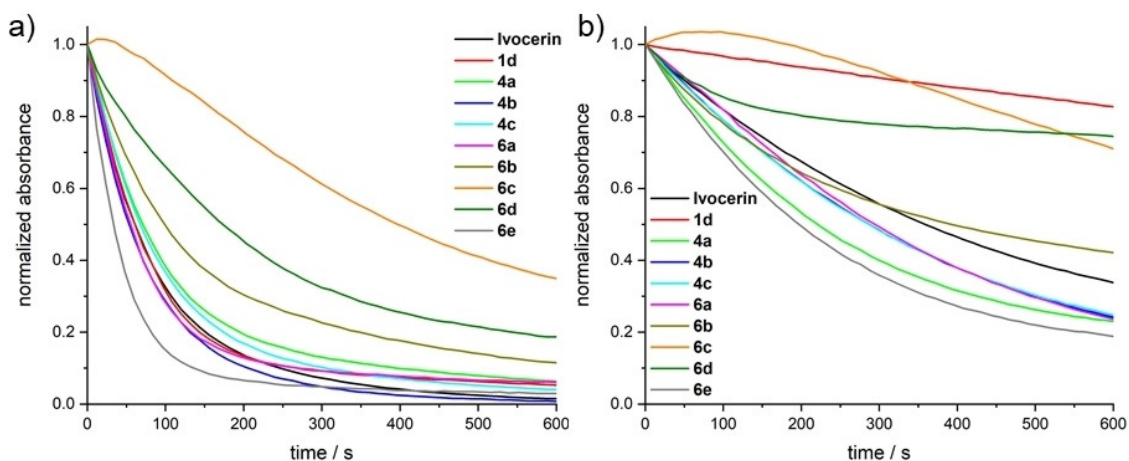
Photobleaching behavior

In applications such as dental restoration, efficient photobleaching is pivotal to avoid the formation of colored polymers. Furthermore, the curing depth also strongly depends on the absorption behavior of the formed polymer: the more effective the discoloration of the PI/monomer reactive mixture, the greater the curing depth.[11, 12, 14–18] Hence, we investigated the photobleaching behavior of the mixed acylgermanes and compared it with already published data.[13, 14]

Degassed solutions of **4a–c** and **6a–e** ($A_{385} \approx 0.6$ to ensure comparability) in toluene/methyl methacrylate (MMA) (1/1 v/v) were irradiated with two different low-power LEDs emitting at wavelengths of 385 and 470 nm (LED385 and LED470; for a detailed description of the LEDs, see Experimental Section and Figure S23 in the Supporting Information), which are typical for dental lamps.[19] The normalized absorbance curves as a function of time are depicted in Figure 3. On irradiation with
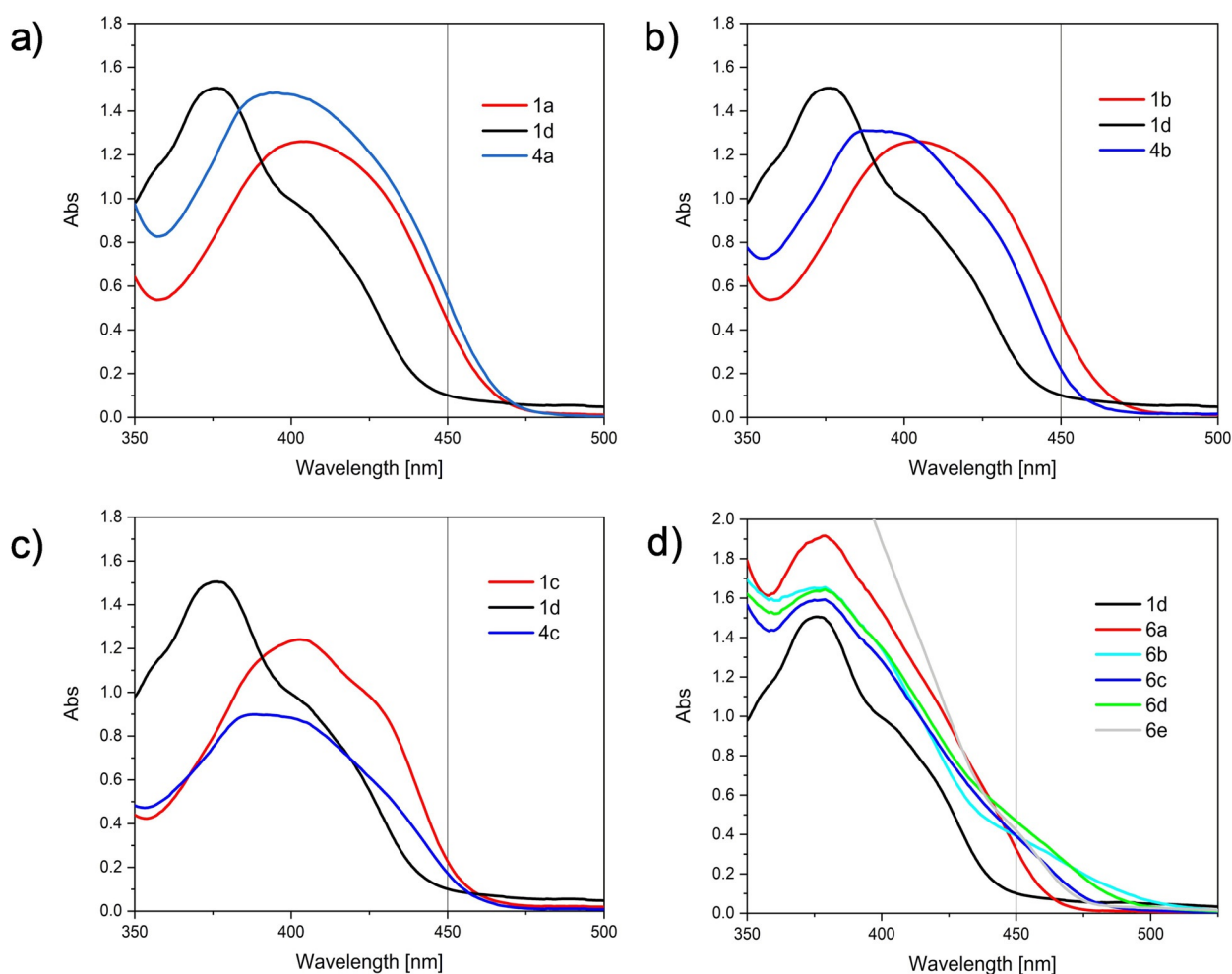
Figure 2. Comparison of the mixed-functionalized tetraacylgermanes with the symmetrical tetraacylgermanes. a) **4a** compared with tetramesitoylgermane and tetrakis(o-toluoyl)germane. b) **4b** compared with tetramesitoylgermane and tetrakis(p-toluoyl)germane. c) **4c** compared with tetramesitoylgermane and tetrabenzoylgermane. d) Mixed-functionalized tetraacylgermanes, synthesized by method B, compared to tetramesitoylgermane (**1d**).

Chemistry–A European Journal

Full Paper
doi.org/10.1002/chem.202004342

**Chemistry
Europe**
European Chemical
Societies Publishing

Figure 3. Steady-state photolysis of Ivocerin, **1 d**, **4 a–c**, and **6 a–e** with a) LED385, b) LED470 in toluene/MMA (1/1 v/v). The absorbance traces are normalized to the initial absorptions at the observation wavelengths (maxima of n/σ–π* transitions; Ivocerin: 412.0 nm; **1 d**: 378.0 nm, **4 a**: 397.0 nm, **4 b**: 400.0 nm, **4 c**: 400.0 nm, **6 a**: 380.0 nm, **6 b**: 379.0 nm, **6 c**: 379.5 nm, **6 d**: 378.0 nm, **6 e**: 373.0 nm). Data for Ivocerin and **1 d** were taken from the literature.[13]

LED 385 (see Figure S25 in the Supporting Information for UV/Vis spectra during illumination), most of the compounds are bleached efficiently in presence of MMA, and only **6 b–d** show slow decay. On irradiation with LED 470 (see Figure S26 in the Supporting Information for UV/Vis spectra during illumination), compounds **4 a–c** and **6 a–e** are bleached more efficiently than tetramesitoylgermane (**1 d**, red line in Figure 3 b) due to their higher absorbance at 470 nm (see Figure 1).

Interestingly, the absorbance for **6 c** initially increases and then slowly decays (orange curves in Figure 3). A shift of the absorption maximum from 379.5 nm for **6 c** to 382 nm is also observable (see Figure S24 in the Supporting Information). These observations point to the formation of a colored photoproduct.

Following the procedure by Stadler et al.,[16] we determined the quantum yield of decomposition for the mixed acylgermanes **4 a–c** and **6 a–e** (Table 1). For **6 e**, which is bleached most efficiently on irradiation with LED 385, the highest quantum yield ($\phi = 0.57$) was measured, followed by **4 a** ($\phi = 0.52$). These values are considerably higher than those of symmetrical tetraacylgermanes (0.34–0.44) found in a previous study.[14] Compounds **6 b** and **6 d**, both featuring an EWG (methyl ester and nitrile, respectively) at the *para* position of the second aroyl substituent, show the lowest quantum yields in the series of compounds.

Table 1. Wavelength of n/σ–π* absorption maxima and extinction coefficients [in toluene/MMA 1/1 (v/v)] and determined quantum yields.

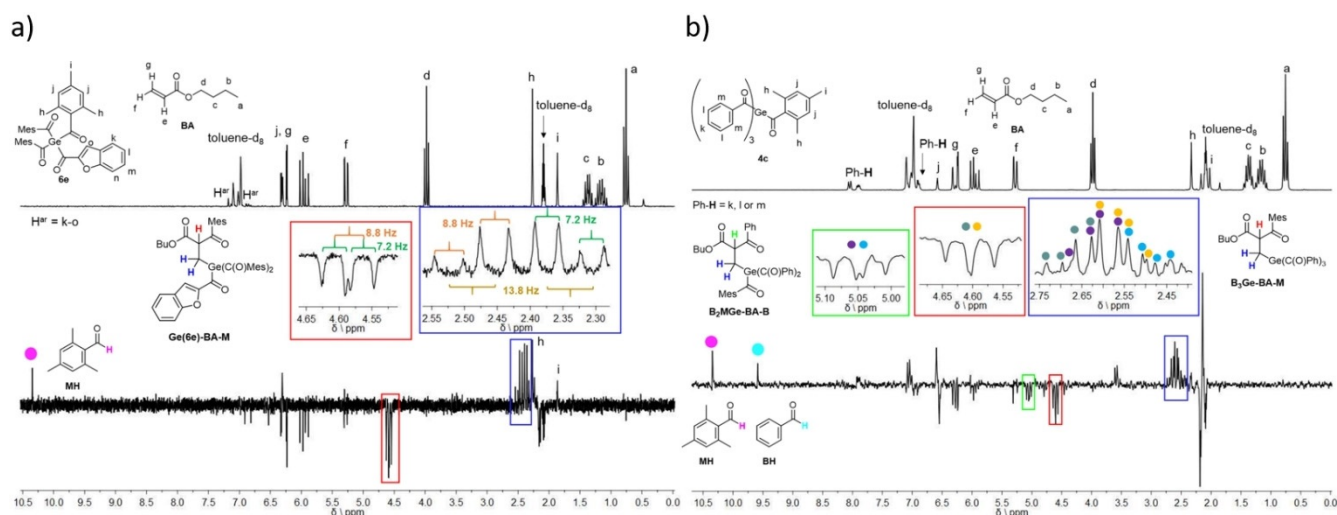|	$\lambda_{max,exptl}$ [nm]	ε [$\mathrm{M^{-1}\,cm^{-1}}$] at $\lambda_{max,exptl}$	ϕ (385 mm)
Ivocerin[a]	412.0	1001	0.86 ± 0.02
1 d[a]	378.0	1839	0.38 ± 0.01
4 a	397.0	1078	0.52 ± 0.01
4 b	400.0	1323	0.48 ± 0.01
4 c	400.0	1363	0.42 ± 0.01
6 a	380.0	1766	0.41 ± 0.01
6 b	379.0	1675	0.24 ± 0.01
6 c	379.5	1656	_[c]
6 d	378.0	1865	0.15 ± 0.01
6 e	373.0[b]	2091	0.57 ± 0.01

[a] Ref. [13]. [b] Shoulder. [c] Not determinable.

CIDNP studies

To elucidate the radical reaction pathways on initiation, the title compounds were investigated by chemically induced dynamic nuclear polarization (CIDNP), an NMR-based technique that allows detection of short-lived intermediates formed from photoinitiators. A remarkable feature of CIDNP NMR spectra of photoinitiators containing aroyl groups is the detection of aldehydes as products of the benzoyl-type primary radicals in the presence of monomers.[12,15,20–22] Therefore, we employed

this technique to determine which of the aroyl groups are cleaved preferentially on UV irradiation ($\lambda = 355$ nm).

The CIDNP spectra of solutions of **1 a**, **1 c**, **1 d**, **4 a–c**, and **6 a–e** in [D8]toluene in the presence of the monomer butyl acrylate (BA) were acquired. For the tri(mesitoyl)aroylgermanes (**6 a–e**) and tetramesitoylgermane **1 d**, the same aldehyde signal was evident, which is assigned to mesitaldehyde (**MH**, $\delta = 10.34$ ppm),[15] as shown in Figure 4 a for **6 e**.

However, this is not the only information that can be extracted from the CIDNP spectra. Furthermore, on the basis of the CIDNP data, the mechanism of the radical addition can be elucidated. The germyl radical formed on cleavage can, in principle, attack both vinyl positions in butyl acrylate (α or β position) to form two regioisomers **R1** and **R2** (see Figure S38 in the Supporting Information). In a further step, both isomers recombine with a mesitoyl radical to form **P1** and **P2**.

In the CIDNP spectrum of **6 e** (Figure 4 a), the signals centered at 4.6 ppm (enclosed in the red rectangle) can be interpreted as a doublet of doublets with $J = 7.2$ and 8.8 Hz. These coupling constants are also found in the multiplet at 2.29–2.55 ppm (blue rectangle), which, in fact, consists of two doublets of doublets with $J = 13.8$ Hz. Such a coupling pattern is

Chemistry–A European Journal

Full Paper
doi.org/10.1002/chem.202004342

Chemistry Europe
European Chemical
Societies Publishing

Figure 4. ^{1}H NMR and CIDNP spectra (excitation at $\lambda = 355$ nm, ca. 50 mJ per pulse) of a) **6e** in the presence of butyl acrylate (5.8 mM **6e**, 50 mM BA in [D$_8$]toluene) and b) **4c** in the presence of butyl acrylate (7.6 mM **4c**, 50 mM BA in [D$_8$]toluene).

typical for a methylene group adjacent to a chiral center. As the difference in chemical shift (ca. 30 Hz) for the methylene protons is in the range of the geminal coupling constant ($^2J = 13.8$ Hz), a second-order effect ("roof effect") in the spectrum is evident.[23]

For both regioisomers **P1** and **P2**, the same coupling pattern is expected; however, on the basis of the chemical shift of the CH signal (4.6 ppm), the proton can be assigned to the α position of two carbonyl groups in **P1** (see Figure S39 in the Supporting Information; see Figure 4a for structure of **Ge(6a)-BA-M**). This regioisomer, formed by attack at the β position, was also postulated in previous publications by us.[12,15] These coupling patterns can also be found in the CIDNP spectra of **6a–d**, **1a**, and **1c**; only for **1d** is it not observable (see Table 2).

In case of the triaroylmesitoylgermanes (**4a–c**), two aldehyde signals are observable [**MH** and o-tolualdehyde (o-TH) for **4a**; **MH** and p-tolualdehyde(p-TH) for **4b**; **MH** and benzaldehyde (**BH**) for **4c**] in the corresponding CIDNP spectra (see Figures S31 and S32 in the Supporting Information and Figure 4b), and this indicates that the corresponding benzoyl-type radicals are formed as intermediates. Moreover, the CIDNP spectra of **4a–c** show more than one signal in the region around 4.5 ppm (CH group) and, in addition, the multiplet around 2.5 ppm (methylene protons) becomes more complicated, as shown for **4c** in Figure 4b. This means that different addition products are formed. The signal enlarged in the red rectangle in Figure 4b can be interpreted as dd ($J = 7.4$ and 8.5 Hz), and for the signal at 5.05 ppm (green rectangle) 6.8 and 8.9 Hz are obtained as coupling constants. With these data in hand, the multiplet enlarged in the blue rectangle can be deconstructed to four dds, as indicated by the colored circles. As the chemical shift and the coupling constants found for the dd at 5.05 ppm are almost identical to the values obtained for **B$_3$Ge-BA-B** formed from **1c** (see Table 2), we expect a similar product, namely **B$_2$MGe-BA-B**, which features a mesitoyl group (M) instead of a benzoyl group (B) at the Ge center.

The stronger signal at 4.60 ppm is attributed to **B$_3$GeBA-M**. Further small signals in the vicinity of the CH and methylene proton signals suggest that additional (similar) photoproducts (e.g., **B$_2$MGe-BA-M**) are formed. These products clearly mirror the reactivity of the primarily formed germyl radicals.

In case of **4b**, three CH signals can be clearly identified (see Table 2, Figure S32 of the Supporting Information); however, only one geminal coupling constant can be extracted from the multiplet at 2.6 ppm. Nevertheless, the dd having the largest chemical shift (5.09–5.17 ppm) might be attributed to (**p-T)$_2$MGe-BA-(p-T)**. If a mesitoyl group is located adjacent to the

Table 2. Chemical shifts and coupling constants for the addition products formed from compounds **1a**, **1c**, **1d**, **4a–c**, and **6a–e** observed in the CIDNP spectra.

Compound	δ(CH$_2$) [ppm]	δ(CH) [ppm] [a]	^3J [Hz]	^2J [Hz]
1a	2.34–2.58	4.80–4.88[b]	8.0	13.5
1c	2.44–2.67	5.01–5.08	7.0, 9.0	13.5
1d	2.29–2.33	4.28–4.35	6.5, 8.0	–[d]
4a	2.30–2.55	4.80–4.88[b]	8.0[c]	–[d]
		4.64–4.72[b]	8.0[c]	–[d]
		4.48–4.56[b]	8.0[c]	–[d]
		4.41–4.49[b]	8.0[c]	–[d]
4b	2.39–2.79	4.65–4.73	7.0, 9.0[c]	13.6
		5.09–5.17	7.0, 8.8[c]	–[d]
		4.45–4.53	7.0, 8.7[c]	–[d]
4c	2.42–2.73	4.56–4.64	7.4, 8.5[c]	13.6
		5.01–5.09	6.8, 8.9[c]	13.4
		4.42–4.50		
		4.76–4.80		
6a	2.18–2.46	4.40–4.48	6.5, 9.3	14.0
6b	2.21–2.48	4.42–4.50	6.5, 9.3	13.7
6c	2.23–2.43	4.27–4.35	7.6, 8.5	14.1
6d	2.17–2.42	4.32–4.40	7.0, 9.0	14.0
6e	2.29–2.55	4.55–4.63	7.2, 8.8	13.8

[a] Sorted from most intense to weakest signals (for **4a–c**). [b] Triplet instead of doublet of doublets. [c] Assigned to the respective signal in the previous column. [d] Not determinable.

Chemistry–A European Journal

Full Paper
doi.org/10.1002/chem.202004342

Chemistry Europe
European Chemical
Societies Publishing

CH group, a smaller chemical shift would be expected (in accordance with the CH shifts observed for **1 d**, **6 a**–**e**). For **4 a**, four signals of almost the same intensity are detected in the region typical for the CH proton (red rectangle in Figure S31 of the Supporting Information). One of the signals coincides with the signal of the CH proton for the photoproduct of **1 a**; hence, the formation of a similar photoproduct is expected. Possible addition products are shown in Figure S31 of the Supporting Information.

Finally, on the basis of the CIDNP data, the question whether the two different aroyl radicals (observed for **4 a-c**) are cleaved from different acylgermane molecules or from the same molecule (i.e., two consecutive cleavages) is answered. In a previous study,[15] it was found that the chemical shift of the methylene protons adjacent to the Ge center is susceptible to the nature of the other substituents at the Ge atom. If alkyl groups are present, a shift to higher field is expected. As the multiplets for **4 a**–**c** are found in the same region as those for **1 c**, **1 d**, and **6 a**–**e** (or even shifted downfield, see Figure S37 of the Supporting Information for comparison), consecutive cleavage (and addition) at the same acylgermane molecule seems unlikely on the timescale of the CIDNP NMR experiment.

Solubility

Low solubility is a huge drawback of symmetrical tetraacylgermanes. On introducing a mixed substitution pattern at the germanium atom of tetraacylgermanes an increase in solubility was observed (see Table 3). For this reason, as well as the broad n–π* absorption bands, a wide variety of applications becomes feasible.

Solubility tests were carried out with MMA, BA, and acetonitrile, and the amounts of the compounds dissolved in 100 μL of solvent were analyzed for methods A (Table 4) and B (Table 5). The results were compared to those of symmetrical tetramesitoylgermane (**1 d**), the data of which can also be

Table 3. Comparison of melting points of symmetrical and mixed-functionalized tetraacylgermanes. Compounds synthesized with method B are compared to tetramesitoylgermane (**1 d**).

Symmetrical	m.p. [°C]	A	m.p. [°C]	B	m.p. [°C]
1 a	123–125[a]	**4 a**	92–96	**6 a**	148–150
1 b	decomp > 230[a]	**4 b**	95–100	**6 b**	106–108
1 c	82.5–83[b]	**4 c**	148–150	**6 c**	190–192
1 d	198–199[b]			**6 d**	208–210
				6 e	168–170

[a] Ref. [14] . [b] Ref. [12]

Table 4. Amount of compound (synthesized with method A) dissolved in 100 μL of the respective solvent compared with **1 d**.

	1 d [mg]	**4 a** [mg]	**4 b** [mg]	**4 c** [mg]
BA	9.70	128	23.3	68.7
MMA	4.80	56.7	18.9	69.9
acetonitrile	0.40	0.80	1.70	23.5

Table 5. Amount of compound (synthesized with method B) dissolved in 100 μL of the respective solvent.

	6 a [mg]	**6 b** [mg]	**6 c** [mg]	**6 d** [mg]	**6 e** [mg]
BA	13.2	77.5	1.20	7.20	4.10
MMA	2.60	114	3.40	1.40	2.90
acetonitrile	1.70	5.30	0.10	0.30	0.80

found in Table 4. The mixed-functionalized tetraacylgermanes synthesized by method A show exceptionally high solubility, especially **4 a**. Switching the methyl group to the *para* position on the benzoyl group leads to lower solubility compared with the compound with the methyl group in the *ortho* position. The compounds synthesized according to method B show a significant decrease in solubility compared with those of method A. This can be attributed to the number of mesitoyl groups in the molecule: the higher the number of mesitoyl substituents, the lower the solubility, and vice versa. Moreover, the solubility of compound **6 b** increases by 1500 % (replacement of a mesitoyl group with a benzoyl group bearing an ester moiety in the *para* position). Even in acetonitrile, which is an unsuitable solvent for the other compounds, a good result could be achieved. We suggest that the reason for this behavior is the presence of the polar ester moiety.

NMR Spectroscopy

NMR spectra and detailed characterization of **4 a**–**c** and **6 a**–**e** are provided in the Experimental Section and the Supporting Information. All compounds show very similar ^{13}C chemical shifts for the carbonyl C atom between 209.22 and 233.36 ppm, which is characteristic for carbonyl groups directly linked to a germanium atom. The presence of two different carbonyl groups characteristic of the unsymmetrical tetraacylgermanes is confirmed by the occurrence of two peaks in this region.

X-Ray crystallography

Crystals suitable for single-crystal XRD were obtained for compounds **4 a**–**c** and **6 a**–**e**. As two representative examples, the molecular structures of **4 a** (method A) and **6 b** (method B) are shown in Figures 5 and 6. All other structures can be found in the Supporting Information.

The torsion angle between the C=O bond and the aromatic plane of the mesitoyl group is much larger than of any other aroyl substituent (Table 6). The bond lengths are slightly elongated compared with the average Ge–C bond (1.97 Å)[24] and the average C=O bond (1.19 Å).[25] The obtained crystallographic data of the mixed derivatives are similar to those of the symmetrical compounds.[13]

Conclusion

We were able to synthesize a variety of mixed-functionalized tetraacylgermanes via two different synthetic routes. Purifica-

Chemistry–A European Journal

Full Paper
doi.org/10.1002/chem.202004342

Chemistry Europe
European Chemical
Societies Publishing
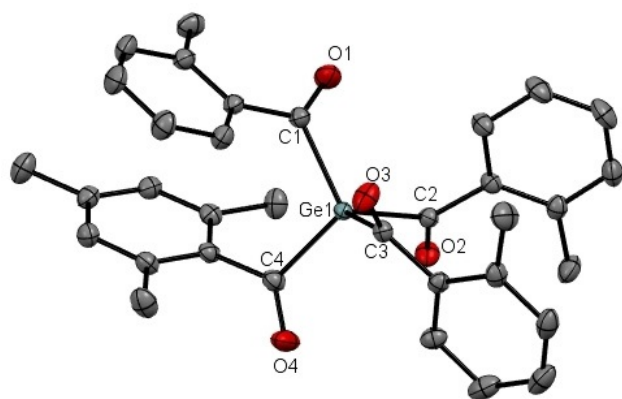
Figure 5. ORTEP of **4 a**. Thermal ellipsoids are depicted at 50 % probability. Hydrogen atoms are omitted for clarity. The torsion angle (mean value) between the C=O group and the aromatic ring plane of the o-toluoyl group is 27.76°. The torsion angle between the C=O group and the aromatic ring plane of the mesitoyl group is 65.40°.
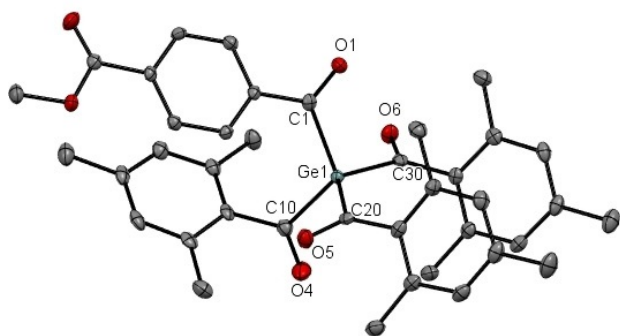
Figure 6. ORTEP of **6 b**. Thermal ellipsoids are depicted at 50 % probability. Hydrogen atoms are omitted for clarity. The torsion angle between the C=O group and the aromatic ring plane of the ester group is 21.41°. The torsion angle (mean value) between the C=O group and the aromatic ring plane of the mesitoyl group is 56.23°.

Table 6. Mean bond lengths d [Å] and torsion angles [°] between the C=O group and the aromatic ring plane of compounds **4 a–c** and **6 a–e**. R^1 represents the mesitoyl substituent, and R^2 the respective acyl group of each compound.

	d_{Ge-C}	$d_{C=O}$ (R^1)	$d_{C=O}$ (R^2)	∡O=C−R^1	∡O=C−R^2
4 a	2.039	1.209	1.225	65.40	27.76
4 b	2.025	1.219	1.215	48.36	8.71
4 c	2.028	1.214	1.216	83.20	8.24
6 a	2.034	1.213	1.217	66.88	18.79
6 b	2.031	1.213	1.218	56.23	21.41
6 c	2.039	1.211	1.212	54.66	29.72
6 d	2.033	1.214	1.217	62.21	13.89
6 e	2.030	1.212	1.219	60.10	4.16

tion by column chromatography is crucial for method A, which reduces the yields of that pathway. Therefore, method B was introduced, with which even EWGs can be introduced. The new mixed-functionalized tetraacylgermanes **4 a–c** and **6 a–e** show lower melting points than symmetrical tetraacylger-

manes. The lower melting points result in improved solubility, which was also confirmed by solubility tests in BA, MMA, and acetonitrile. The introduction of mixed functionality into tetraacylgermanes leads to broadening of their absorption band with an increased absorption maximum. Curing of formulations containing Ivocerin is problematic with light of wavelength above 450 nm, but the synthesized mixed tetraacylgermanes show high absorption even in this range. Remarkably, tailing of the absorption spectrum up to 525 nm was observed.

Photobleaching experiments showed that all compounds except **6 b–d** are bleached efficiently on illumination with a 385 nm LED. Due to the higher absorption at wavelengths above 450 nm, solutions of **4 a–c**, **6 a** and **6 e** are bleached significantly faster than Ivocerin and the symmetrical tetraacylgermane **1 d** when irradiated with LED 470. This opens up the possibility of efficient curing with visible-light sources, which is of high importance for medical applications. The highest quantum yield in the series of compounds was found for **6 e** ($\phi=$ 0.57).

The reaction pathways of the primary radicals (germyl and benzoyl) were investigated by CIDNP NMR spectroscopy. For the trimesitoylaroylgermanes **6 a–e** the same aldehyde signal as for tetramesitoylgermane (**1 d**) was detected, which indicated that only the mesitoyl group is cleaved off in **6 a–e**. The triaroylmesitoylgermanes **4 a–c** feature two aldehyde signals in their CIDNP spectra suggesting that α-cleavage can happen at both the aroyl group (o-toluoyl in **4 a**, p-toluoyl in **4 b**, and benzoyl in **4 c**) and the mesitoyl group. On the basis of the coupling patterns seen for the signals in the regions of 2.2–2.8 and 4.3–5.2 ppm in the CIDNP spectra, which are observed for all compounds (except for **1 d**), regioselective addition of the germyl radical to the β position of the monomer butyl acrylate, in accordance with previous observations,[12,15] can be suggested.

Further studies to probe the scope of these initiators are currently in progress.

Experimental Section

General considerations

All synthetic steps were performed under inert conditions by using standard Schlenk techniques. Solvents were dried with a column solvent purification system.[26] Commercial acid chlorides, benzoyl fluoride, and KOtBu were used without further purification. Tetrakis(trimethylsilyl)germane [(Me₃Si)₄Ge],[27,28] tetramesitoylgermane (GeMes₄),[12] and the acid fluorides[29] were produced according to the corresponding literature. ¹H (299.95 MHz), ¹³C (75.43 MHz), and ²⁹Si (59.59 MHz) NMR spectra were recorded with a Varian INOVA 300 spectrometer in CDCl₃ solution and were referenced versus TMS by using the internal ²H lock signal of the solvent. UV/Vis spectra were recorded with an Agilent Cary 60 UV/VIS spectrometer.

Synthesis

Mesitoyltri(trimethylsilyl)germane (2): Compound **2** was synthesized according to the literature.[12] Ge(SiMe₃)₄ (5.0 g, 13.7 mmol, 1.0 equiv) was dissolved in dry DME (30 mL). KOtBu (15.1 mmol,

Chemistry–A European Journal

Full Paper
doi.org/10.1002/chem.202004342

Chemistry Europe
European Chemical
Societies Publishing

1.1 equiv) was added at RT and the mixture stirred for 20 min. The solution was added slowly at 0 °C with a syringe pump to a solution of mesitoyl chloride (2.5 mL, 15.1 mmol, 1.1 equiv) in diethyl ether (60 mL). After complete addition, the slightly orange solution was warmed to RT. After aqueous workup with saturated NH_4Cl the phases were separated and the aqueous phase was extracted with dichloromethane (3×). The combined organic layers were dried over Na_2SO_4, filtered, and the volatile components were evaporated. The product was isolated by flash column chromatography (heptane/toluene 1:1). The slightly yellow, crystalline product was isolated in 58% yield (3.46 g). ^1H NMR (300 MHz, $CDCl_3$): $\delta = 6.75$ (s, 2H, Mes-*H*), 2.25 (s, 3H, Mes-*p*C*H*₃), 2.15 (s, 6H, Mes-*o*C*H*₃), 0.21 ppm (s, 27H, SiMC*H*₃); ^{13}C NMR (75 MHz, $CDCl_3$): $\delta = 247.93$ (Ge*C*OMes), 147.30 (Mes-*C*), 137.49 (Mes-*C*), 130.25 (Mes-*C*), 128.62 (Mes-*C*), 21.08 (Mes-*p*C*H*₃), 19.41 ppm (Mes-*o*C*H*₃); ^{29}Si NMR (60 MHz, $CDCl_3$, ppm): $\delta = -5.06$ ppm (*Si*Me₃).

Mesitoyltri(o-toluoyl)germane (4a): A flask was charged with compound **2** (1.00 g, 2.28 mmol, 1.0 equiv) and KO*t*Bu (0.28 g, 2.50 mmol, 1.1 equiv), dry DME (10 mL) was added, and the solution was stirred for 30 min. In a second flask, *o*-toluoyl fluoride (0.97 mL, 8.93 mmol, 3.1 equiv) was dissolved in dry DME (10 mL) and the solution cooled to 0 °C. The solution of the anion was added slowly to the solution of *o*-toluoyl fluoride through a syringe. The solution was stirred for 12 h at RT. After aqueous workup with saturated NH_4Cl, the phases were separated and the aqueous phase was extracted three times with dichloromethane. The organic layer was dried over Na_2SO_4, filtered, and the solvent was removed by rotatory evaporation. The crude product was re-condensed and further recrystallized from acetonitrile to give 0.50 g (48%) of pure slightly yellow, crystalline product. M.p. 92–96 °C; UV/Vis (acetonitrile): $\lambda = 396$ nm, $\varepsilon = 1483$ L mol⁻¹ cm⁻¹; IR: $\tilde{v}$/cm⁻¹ = 1630, 1607, 1562, 1555 (m, $v_{C=O}$); elemental analysis (%) calcd for $C_{34}H_{32}GeO_4$: C 70.74, H 5.59%; found: C 70.77, H 5.53; ^1H NMR (300 MHz, $CDCl_3$): $\delta = 7.64$ (d, 3H, *J* = 7.43 Hz, Ph-*H*), 7.24–7.12 (m, 9H, Ph-*H*), 6.53 (s, 2H, Mes-*H*), 2.42 (s, 9H, Ph-*o*C*H*₃), 2.12 (s, 3H, Mes-*p*C*H*₃), 2.09 ppm (s, 6H, Mes-*o*C*H*₃); ^{13}C NMR (75 MHz, $CDCl_3$): $\delta = 233.36$ (Ge*C*OMes), 224.57 (Ge*C*O*o*-Tol), 141.92 (Mes-*C*), 139.81 (*o*-Tol-*C*), 139.64 (Mes-*C*), 137.30 (*o*-Tol-*C*), 133.23 (*o*-Tol-*C*), 132.43 (Mes-*C*), 132.03 (*o*-Tol-*C*), 131.90 (*o*-Tol-*C*), 128.89 (Mes-*C*), 125.88 (*o*-Tol-*C*), 21.10 (Mes-*p*C*H*₃), 21.03 (*o*-Tol-*C*H₃), 19.19 ppm (Mes-*o*C*H*₃).

Mesitoyltri(p-toluoyl)germane (4b): Compound **2** (1.0 g, 2.28 mmol, 1.0 equiv) and KO*t*Bu (0.27 g, 2.50 mmol, 1.05 equiv) were dissolved in dry DME (10 mL). The mixture was stirred for 30 min. The potassium germanide was added dropwise by syringe to a second flask, charged with *p*-toluoyl fluoride (0.74 mL, 8,64 mmol, 3.0 equiv) in dry DME (10 mL). After reaching RT, the solution was stirred for a further 12 h, followed by aqueous workup with NH_4Cl, extraction with dichloromethane, drying over Na_2SO_4, filtration and removal of the solvent under reduced pressure. The product was further purified by column chromatography, yielding 0.48 g (45%) of slightly yellow crystals. M.p. 95–100 °C; UV/Vis (acetonitrile): $\lambda = 387$ nm, $\varepsilon = 1310$ L mol⁻¹ cm⁻¹; IR: $\tilde{v}$/cm⁻¹ = 1624, 1593 (m, $v C=O$), elemental analysis (%) calcd for $C_{34}H_{32}GeO_4$: C 70.37, H 5.59; found: C 70.50, H 5.30; ^1H NMR (300 MHz, $CDCl_3$): $\delta = 8.05$ (d, 6H, *J* = 8.41 Hz, Aryl-*H*), 7.54 (d, 6H, *J* = 7.36 Hz, Aryl-H), 6.99 (s, 2H, Mes-*H*), 2.71 (s, 9H, Ph-*p*C*H*₃), 2.53 (s, 6H, Mes-*o*C*H*₃), 2.51 ppm (s, 3H, Mes-*p*C*H*₃); ^{13}C NMR (75 MHz, $CDCl_3$): $\delta = 232.44$ (Ge*C*OMes), 220.72 (Ge*C*OAryl), 145.11 (Aryl-*C*), 141.93 (Mes-*C*), 139.86 (Mes-*C*), 138.18 (Aryl-*C*), 132.77 (Mes-*C*), 129.53 (Aryl-*C*), 129.36 (Aryl-*C*), 128.88 (Mes-*C*), 21.77 (Aryl-*p*C*H*₃), 21.06 (Mes-*p*C*H*₃), 19.31 ppm (Mes-*o*C*H*₃).

Mesitoyltribenzoylgermane (4c): A flask was charged with compound **2** (1.0 g, 2.28 mmol 1.0 equiv) and KO*t*Bu (0.27 g, 2.50 mmol, 1.05 equiv). After dissolving in dry DME (10 mL), the reaction mixture was stirred for 30 min. In a second flask, benzoyl fluoride (0.74 mL, 8.64 mmol, 3.0 equiv) was dissolved in dry DME (10 mL) and cooled to 0 °C. The potassium germanide solution was added dropwise to the benzoyl fluoride solution. After heating to RT, the reaction mixture was stirred for a further 12 h. After aqueous workup with NH_4Cl, the aqueous phase was extracted with dichloromethane (3×). The organic layer was dried over Na_2SO_4, filtered, and the solvent was removed under reduced pressure. The product was further purified by column chromatography, yielding 0.63 g (52%) of yellow crystals. M.p. 148–150 °C; UV/Vis (acetonitrile): $\lambda = 393$ nm, $\varepsilon = 1310$ L mol⁻¹ cm⁻¹; IR: $\tilde{v}$/cm⁻¹ = 1633, 1581 (m, $v_{C=O}$); elemental analysis (%) calcd for $C_{31}H_{26}GeO_4$: C 69.57, H 4.90; found: C 69.47, H 5.03; ^1H NMR (300 MHz, $CDCl_3$): $\delta = 7.77$–7.74 (m, *J* = 7.18, Hz, 6H, Ph-*H*), 7.47 (dd, 3H, Ph-*H*), 7.36 (m, 6H, Ph-*H*), 6.59 (s, 2H, Mes-*H*), 2.13 ppm (s, 9H, Mes-C*H*₃); ^{13}C NMR (75 MHz, $CDCl_3$): $\delta = 231.58$ (Ge*C*OMes), 221.45 (Ge*C*OPh), 141.82 (Mes-*C*), 140.26 (Ph-*C*), 140.07 (Mes-*C*), 134.02 (Ph-*C*), 132.73 (Mes-*C*), 129.13 (Ph-*C*), 128.99 (Mes-*C*), 128.86 (Ph-*C*), 21.06 (Mes-*p*C*H*₃), 19.28 ppm (Mes-*o*C*H*₃).

p-Bromobenzoyltrimesitoylgermane (6a): A flask was charged with Ge(SiMe₃)₄ (1.0 g, 2.74 mmol, 1.0 equiv) and KO*t*Bu (1.1 g, 3.01 mmol, 1.1 equiv), which were dissolved in 35 mL dry DME. The reaction mixture was stirred for 1 h. Subsequently mesitoyl fluoride (3×0.45 g, in total 8.21 mmol, 3.0 equiv) was added, and after each addition the reaction mixture was stirred for 10 min. After complete addition, the reaction was stirred mixture for a further 2 h. Afterwards, the solution was added slowly to a second flask charged with *p*-bromobenzoyl chloride (2.87 mmol, 1.05 equiv) in toluene (20 mL) at −30 °C and stirred at this temperature for 30 min. The solution was stirred for a further 12 h at RT. After aqueous workup with saturated NH_4Cl, the phases were separated and the aqueous phase was extracted three times with dichloromethane. The organic layer was dried over Na_2SO_4, filtered, and the solvent was removed under reduced pressure. The crude product was recrystallized from acetone to yield 0.45 g (86%) of yellow crystals. M.p. 148–150 °C; UV/Vis (acetonitrile): $\lambda = 379$ nm, $\varepsilon = 1916$ L mol⁻¹ cm⁻¹; IR: $\tilde{v}$/cm⁻¹ = 1647, 1630, 1622, 1606, 1578, 1562 (m, $vC=O$); elemental analysis (%) calcd for $C_{37}H_{37}BrGeO_4$: C 63.65, H 5.34; found: C 63.36%, H 5.21; ^1H NMR (300 MHz, $CDCl_3$): $\delta = 7.52$ (d, *J* = 8.5 Hz, 2H, Aryl-*H*), 7.36 (d, *J* = 8.5 Hz, 2H, Aryl-*H*), 6.56 (s, 6H, Mes-*H*), 2.20 (s, 9H, Mes-*p*C*H*₃), 2.11 ppm (s, 18H, Mes-*o*C*H*₃); ^{13}C NMR (75 MHz, $CDCl_3$): $\delta = 232.24$ (Ge*C*OMes), 220.50 (Ge*C*OAryl), 141.27 (Mes-*C*), 140.08 (Mes-*C*), 138.56 (Aryl-*C*), 133.06 (Mes-*C*), 132.49, 132.03, 131.70 (Aryl-*C*), 130.31 (Aryl-*C*), 128.87 (Mes-*C*), 128.80 (Aryl-C), 21.26 (Mes-*o*C*H*₃), 19.32 ppm (Mes-*p*C*H*₃).

4-Methylbenzoyltetrimesitoylgermane (6b): Germenolate **5** was synthesized by charging a flask with Ge(SiMe₃)₄ (3.0 g, 8.21 mmol, 1.0 equiv) and KO*t*Bu (1.1 g, 9.03 mmol, 1.1 equiv) in dry DME (35 mL). The reaction mixture was stirred for 1 h. Subsequently, mesitoyl fluoride (3×1.36 g, in total 24.63 mmol, 3.0 equiv) was added, and after each addition the reaction mixture was stirred for 10 min. After complete addition, the reaction mixture was stirred for a further 2 h. The solution of the germenolate was added dropwise to a solution of methyl-4-(chlorocarbonyl) benzoate (1.71 g, 8.62 mmol, 1.05 equiv) in toluene (60 mL) at −30 °C by syringe. After complete addition the reaction mixture was allowed to warm to room temperature. After aqueous workup with NH_4Cl, the separated organic layer was dried over Na_2SO_4, filtered, and the solvent was removed under reduced pressure. The crude product was recrystallized from pentane to yield 5.29 g (95%) of yellow crystals.

Chemistry–A European Journal

Full Paper
doi.org/10.1002/chem.202004342

Chemistry Europe
European Chemical
Societies Publishing

M.p. 106–108 °C; UV/Vis (acetonitrile): $\lambda = 378$ and 426 nm (sh), $\varepsilon = 1594$ and 751 (sh) $L\,mol^{-1}\,cm^{-1}$; IR: $\tilde{\nu}/cm^{-1} = 1720$, 1643, 1629, 1606 (m, $\nu C=O$); elemental analysis (%) calcd for $C_{39}H_{40}GeO_6$: C 69.15, H 5.95; found: C 69.13, H 5.98; ^1H NMR (300 MHz, $CDCl_3$): $\delta = 7.90$–7.87 (d, $J = 8.1$ Hz, 2H, Aryl-H), 7.70 (d, $J = 8.1$ Hz, 2H, Aryl-H), 6.56 (s, 6H, Aryl-H), 3.94 (s, 3H, CH_3O), 2.17 (s, 9H, pCH_3), 2.11 ppm (s, 18H, oCH_3); ^{13}C NMR (75 MHz, $CDCl_3$): $\delta = 231.97$, 222.07 ($GeC=O$), 166.25 ($C=O$) 142.63, 141.36, 140.06, 133.59, 133.09, 129.58, 128.83, 128.67 (Aryl-C), 52.60 (CH_3O), 21.20 (Aryl-pCH_3), 19.34 ppm (Aryl-oCH_3).

Synthesis of dioxodihydrobenzofurantrimesitoylgermane (6c): A flask was charged with $Ge(SiMe_3)_4$ (3.0 g, 8.21 mmol, 1.0 equiv) and KOtBu (1.1 g, 9.03 mmol, 1.1 equiv) in dry DME (35 mL). The reaction mixture was stirred for 1 h. Subsequently mesitoyl fluoride (3× 1.36 g, in total 24.63 mmol, 3.0 equiv) were added, and after each addition the reaction mixture was stirred for 10 min. After complete addition, the reaction mixture was stirred for another 2 h. The synthesized germenolate **5** was added dropwise to a solution of 1,3-dioxo-1,3-dihydro-2-benzofuran-5-carbonyl chloride (1.82 g, 8.62 mmol, 1.05 equiv) in toluene (60 mL) at -30 °C by syringe. After allowing the reaction to warm to room temperature, aqueous workup with NH_4Cl followed. The separated organic layer was dried over Na_2SO_4, filtered, and the volatile components removed under reduced pressure. After recrystallization from pentane, pure **6c** was isolated (yellow crystals, 4.81 g, 85%). M.p. 190–192 °C; UV/Vis (acetonitrile): $\lambda = 379$ and 434 nm (sh), $\varepsilon = 1600$ and 506 $L\,mol^{-1}\,cm^{-1}$ (sh); IR: $\tilde{\nu}/cm^{-1} = 1853$, 1782, 1646, 1633, 1605 (m, $\nu C=O$); elemental analysis (%) calcd for $C_{39}H_{36}GeO_7$: C 67.95, H 5.26; found: C 67.98, H 5.29; ^1H NMR (300 MHz, $CDCl_3$): $\delta = 8.25$ (s, 1H, Aryl-H), 8.12–8.09 (d, 1H, Aryl-H), 7.90–7.87 (d, 1H, Aryl-H), 6.55 (s, 6H, Aryl-H), 2.17 (s, 9H, pCH_3), 2.13 ppm (s, 18H, oCH_3); ^{13}C NMR (75 MHz, $CDCl_3$, ppm): $\delta = 230.39$, 222.49 ($GeC=O$), 162.02, 161.42 ($C=O$), 145.42, 141.05, 140.39, 134.52, 133.22, 131.35, 128.98, 126.44, 125.61, (Aryl-C), 21.22 (Aryl-pCH_3), 19.33 ppm (Aryl-oCH_3).

Cyanophenyltrimesitoylgermane (6d): A flask was charged with $Ge(SiMe_3)_4$ (1.0 g, 2.74 mmol, 1.0 equiv) and KOtBu (1.1 g, 3.01 mmol, 1.1 equiv) in dry DME (35 mL). The reaction mixture was stirred for 1 h. Subsequently mesitoyl fluoride (3×0.45 g, in total 8.21 mmol, 3.0 equiv) was added, and after each addition the reaction mixture was stirred for 10 min. After complete addition, the reaction mixture was stirred for a further 2 h. The synthesized germenolate **5** was added dropwise to a solution of 4-cyanobenzoyl chloride (2.87 mmol, 1.05 equiv) in toluene (20 mL) at -30 °C by syringe. After allowing the reaction mixture to warm to room temperature, aqueous workup with NH_4Cl followed. The separated organic layer was dried over Na_2SO_4, filtered, and the solvent was removed under reduced pressure. After recrystallization from pentane, pure dark yellow crystals (1.66 g, 94%) were isolated. M.p. 208–210 °C; UV/Vis (acetonitrile): $\lambda = 379$ nm, $\varepsilon = 1644\ L\,mol^{-1}\,cm^{-1}$; IR $\tilde{\nu}/cm^{-1}$: 1647, 1628, 1606, 1599, 1566, 1562 (m, $\nu C=O$); elemental analysis (%) calcd for $C_{38}H_{37}GeNO_4$: C 70.83, H 5.79, N 2.17; found: C 70.56, H 5.78, N 2.09; ^1H NMR (300 MHz, $CDCl_3$): $\delta = 7.77$–7.74 (d, $J = 8.1$ Hz, 2H, Aryl-H), 7.54–7.51 (d, $J = 8.2$ Hz, 2H, Aryl-H), 6.57 (s, 6H, Mes-H), 2.21 (s, 9H, Mes-pCH_3), 2.11 ppm (s, 18H, Mes-oCH_3); ^{13}C NMR (75 MHz, $CDCl_3$) $\delta = 231.37$ ($GeCOMes$), 221.97 ($GeCOAryl$), 142.15, 141.20, 140.30, 133.11, 132.15, 128.99, 128.86, 117.95, 115.99, (Aryl-C), 21.27 (Mes-pCH_3), 19.34 ppm (Mes-oCH_3).

Benzofurantrimesitoylgermane (6e): A flask was charged with $Ge(SiMe_3)_4$ (1.0 g, 2.74 mmol, 1.0 equiv) and KOtBu (1.1 g, 3.01 mmol, 1.1 equiv) in dry DME (35 mL). The reaction mixture was stirred for 1 h. Subsequently mesitoyl fluoride (3×0.45 g, in total 8.21 mmol, 3.0 equiv) were added, and after each addition the reaction mixture was stirred for 10 min. After complete addition,

the reaction mixture was stirred for a further 2 h. The solution of synthesized germenolate **5** was added dropwise to a solution of benzofuran-2-carbonyl chloride (2.87 mmol, 1.05 equiv) in toluene (20 mL) at -30 °C by syringe. After allowing the reaction to warm up to room temperature, an aqueous workup with NH_4Cl followed. The separated organic layer was dried over Na_2SO_4, filtered, and the solvent was removed under reduced pressure. After recrystallization from pentane, pure **6e** (1.23 g, 68%) was isolated. M.p. 168–170 °C; UV/Vis (acetonitrile): $\lambda = 379$ nm, $\varepsilon = 2818\ L\,mol^{-1}\,cm^{-1}$ (sh); IR $\tilde{\nu}/cm^{-1}$: 1655, 1642, 1606, 1536 (m, $\nu C=O$); elemental analysis (%) calcd for $C_{39}H_{38}GeO_5$: C 71.04, H 5.81% H; found: C 70.80, H 5.61; ^1H NMR (300 MHz, $CDCl_3$) $\delta = 7.60$ (d, $J = 7.8$ Hz, 1H, Aryl-H), 7.50–7.45 (m, 1H, Aryl-H), 7.39–7.36 (d, $J = 8.4$ Hz, 1H, Aryl-H), 7.31 (s, 1H, Aryl-H), 7.28 (s, 1H, Aryl-H), 6.60 (s, 6H, Mes-H), 2.18 (s, 18H, Mes-oCH_3), 2.13 ppm (s, 9H, Mes-pCH_3); ^{13}C NMR (75 MHz, $CDCl_3$) $\delta = 230.90$ ($GeCOMes$), 209.22 ($GeCOAryl$), 155.59, 154.63, 141.27, 140.02, 133.20, 128.87, 126.99, 124.03, 123.99, 112.61, (Aryl-C), 21.16 (Mes-oCH_3), 19.32 ppm (Mes-pCH_3).

CIDNP NMR spectroscopy

CIDNP NMR experiments were carried out with a 200 MHz Bruker AVANCE DPX spectrometer equipped with a custom-made CIDNP probe head. A Quantel Nd-YAG Brilliant B laser (355 nm, ca. 50 mJ per pulse, pulse length 8–10 ns) operating at 20 Hz was employed as light source. The pulse sequence of the experiment consisted of a series of 180° radio-frequency (RF) pulses to suppress the NMR signals of the parent compounds, the laser flash, the 90° RF detection pulse, and the acquisition of the free induction decay. "Dummy" CIDNP spectra, acquired by employing the same pulse sequence but without the laser pulse, were always measured. Samples were prepared in $[D_8]$toluene and deoxygenated by bubbling with nitrogen before the experiment. Chemical shifts δ are reported in ppm relative to TMS by using the residual methyl signal of deuterated toluene as an internal reference ($\delta_H = 2.09$ ppm). If necessary, line broadening (1 Hz, exponential) was applied to the spectra.

Steady-state photolysis and determination of quantum yields

UV/Vis spectra were acquired with a TIDAS UV/Vis spectrometer equipped with optical fibers and a 1024-pixel diode-array detector (J&M Analytik AG, Essingen, Germany). For the photobleaching experiments, two different LEDs (Roithner Lasertechnik GmbH, Vienna, Austria) were used: LED 385 (emission maximum 387 nm; 15 nm full width at half-maximum; 7.8 mW at 20 mA) and LED 470 (emission maximum at 463 nm; 30 nm full width at half-maximum; 7.4 mW at 20 mA). The output power of the LEDs was determined by a spectrophotometer (GL Spectis, GL Optics, Germany) equipped with an integrating sphere (Ulbricht sphere). Both LEDs were operated at a photon flux of 0.05 $\mu mol\,s^{-1}$ to ensure comparability of the results. Solutions of the investigated compounds in a 1:1 (v:v) mixture of toluene and methyl methacrylate (MMA) were filled into 1×1 cm quartz cuvettes intended for fluorescence measurements and degassed by bubbling with argon for 5 min. Samples were irradiated perpendicular to the optical path of the spectrometer and stirred during the measurements with a magnetic stirring bar (750 rpm). The concentrations of the compounds were between 0.34 and 0.65 mM (within the linear range of the spectrometer). The data acquired in the photobleaching experiment with LED 385 were used to determine the quantum yields of decomposition. To that end, the absorbance traces were converted to concentration traces and fitted with a mono-exponential function.

The setup and method are described in more detail in the literature.[16]

Crystallographic data

Deposition numbers 2024318 (**4a**), 2024319 (**4b**), 2024320 (**4c**), 2024321 (**6a**), 2024322 (**6b**), 2024323 (**6c**), 2024324 (**6d**), and 2024325 (**6e**) contain the supplementary crystallographic data for this paper. These data are provided free of charge by the joint Cambridge Crystallographic Data Centre and Fachinformationszentrum Karlsruhe Access Structures service.

Acknowledgements

Conflict of interest

The authors declare no conflict of interest.

[1] L. R. Gatechair, D. Wostratzky in *Adhesive Chemistry: Developments and Trends, Vol. 2* (Ed.: L.-H. Lee), Springer, Boston, **1985**, p. 409.
[2] A. Bagheri, J. Jin, *ACS Appl. Polym. Mater.* **2019**, *1*, 593.
[3] H.-B. Sun, S. Kawata in *NMR 3D Analysis Photopolymerization, Vol. 170*, Springer, Heidelberg, **2004**, p. 169.
[4] I. V. Khudyakov, M. B. Purvis, N. J. Turro, in *Photoinitiated Polymerization, Vol. 847*, American Chemical Society, Washington, D.C., **2003**, p. 113.
[5] N. Moszner, U. Salz, *Prog. Polym. Sci.* **2001**, *26*, 535.
[6] A. Santini, I. T. Gallegos, C. M. Felix, *Prim. Dent. J.* **2013**, *2*, 30.
[7] Y. Yagci, S. Jockusch, N. J. Turro, *Macromolecules* **2010**, *43*, 6245.
[8] J.-P. Fouassier, F. Morlet-Savary, J. Lalevée, X. Allonas, C. Ley, *Materials* **2010**, *3*, 5130.
[9] L. Gonsalvi, M. Peruzzini, *Angew. Chem. Int. Ed.* **2012**, *51*, 7895; *Angew. Chem.* **2012**, *124*, 8017.
[10] N. Moszner, F. Zeuner, I. Lamparth, U. K. Fischer, *Macromol. Mater. Eng.* **2009**, *294*, 877.

[11] B. Ganster, U. K. Fischer, N. Moszner, R. Liska, *Macromolecules* **2008**, *41*, 2394.
[12] J. Radebner, A. Eibel, M. Leypold, C. Gorsche, L. Schuh, R. Fischer, A. Torvisco, D. Neshchadin, R. Geier, N. Moszner, R. Liska, G. Gescheidt, M. Haas, H. Stueger, *Angew. Chem. Int. Ed.* **2017**, *56*, 3103; *Angew. Chem.* **2017**, *129*, 3150.
[13] P. Frühwirt, A. Knoechl, M. Pillinger, S. M. Müller, P. T. Wasdin, R. C. Fischer, J. Radebner, A. Torvisco, N. Moszner, A.-M. Kelterer, T. Griesser, Georg Gescheidt, M. Haas, *Inorg. Chem.* **2020**, *59*, 15204–15217.
[14] J. Radebner, M. Leypold, A. Eibel, J. Maier, L. Schuh, A. Torvisco, R. Fischer, N. Moszner, G. Gescheidt, H. Stueger, M. Haas, *Organometallics* **2017**, *36*, 3624.
[15] A. Eibel, J. Radebner, M. Haas, D. E. Fast, H. Freißmuth, E. Stadler, P. Faschauner, A. Torvisco, I. Lamparth, N. Moszner, H. Stueger, G. Gescheidt, *Polym. Chem.* **2018**, *9*, 38.
[16] E. Stadler, A. Eibel, D. Fast, H. Freißmuth, C. Holly, M. Wiech, N. Moszner, G. Gescheidt, *Photochem. Photobiol. Sci.* **2018**, *17*, 660.
[17] M. Haas, J. Radebner, A. Eibel, G. Gescheidt, H. Stueger, *Chem. Eur. J.* **2018**, *24*, 8258.
[18] N. Moszner, U. K. Fischer, I. Lamparth, P. Fässler, J. Radebner, A. Eibel, M. Haas, G. Gescheidt, H. Stueger, *J. Appl. Polym. Sci.* **2018**, *135*, 46115.
[19] *Scientific Documentation Bluephase Family—LED for Every Use*; Ivoclar Vivadent: Schaan, Liechtenstein.
[20] U. Kolczak, G. Rist, K. Dietliker, J. Wirz, *J. Am. Chem. Soc.* **1996**, *118*, 6477.
[21] M. Griesser, D. Neshchadin, K. Dietliker, N. Moszner, R. Liska, G. Gescheidt, *Angew. Chem. Int. Ed.* **2009**, *48*, 9359; *Angew. Chem.* **2009**, *121*, 9523.
[22] D. Neshchadin, A. Rosspeintner, M. Griesser, B. Lang, S. Mosquera-Vazquez, E. Vauthey, V. Gorelik, R. Liska, C. Hametner, B. Ganster, R. Saf, N. Moszner, G. Gescheidt, *J. Am. Chem. Soc.* **2013**, *135*, 17314.
[23] M. Hesse, H. Meier, B. Zeeh, *Spektroskopische Methoden in der organischen Chemie: 102 Tabellen*, Thieme, Stuttgart, **2005**.
[24] K. M. Baines, W. G. Stibbs, *Coord. Chem. Rev.* **1995**, *145*, 157.
[25] M. Palusiak, S. Simon, M. Solà, *J. Org. Chem.* **2006**, *71*, 5241.
[26] A. B. Pangborn, M. A. Giardello, R. H. Grubbs, R. K. Rosen, F. J. Timmers, *Organometallics* **1996**, *15*, 1518.
[27] A. G. Brook, F. Abdesaken, H. Söllradl, *J. Organomet. Chem.* **1986**, *299*, 9.
[28] H. Bürger, U. Goetze, *Angew. Chem. Int. Ed. Engl.* **1968**, *7*, 212; *Angew. Chem.* **1968**, *80*, 192.
[29] *Methoden der organischen Chemie* (Eds.: B. Baasner, J. L. Adcock, J. Houben, E. Müller, T. Weyl, H. Kropf, K. H. Büchel, O. Bayer), Thieme, Stuttgart **1999**.